MS-NADNet: A Multi-Stream Noise-Aware Deep Learning Framework for Microarray Image Denoising

Shreenidhi B S, R Saravana Kumar
Dayananda Sagar Academy of Technology and Management, Visvesvaraya Technological University, Belagavi, 590018, India
E-mail: shreenidhibs@dsatm.edu.in, saravanakumar.rsk28@gmail.com

Keywords: Microarray imaging, Image denoising, deep learning, multi-stream network, noise characterization, biomedical image processing, MS-NADNet

Received: September 18, 2025

Microarray imaging is a critical tool for large-scale gene expression analysis, yet its accuracy is often compromised by noise introduced during sample preparation, hybridization, and image acquisition. Traditional denoising approaches, including median, Wiener, and wavelet-based filtering, either rely on fixed parameters or degrade under mixed-noise conditions, while CNN-based methods treat all noise uniformly, limiting adaptability. To address these limitations, we propose MS-NADNet (Multi-Stream Noise-Aware Denoising Network), a deep-learning framework that integrates a Noise Characterization Module (NCM) to identify noise type, a set of Noise-Specific Denoising Modules (NSDMs) specialized for distinct noise distributions, and a Global Refinement Block for residual suppression. A large-scale augmented dataset was constructed from the Malignant Lymphoma Classification dataset, incorporating 17 noise variants, including Gaussian, Poisson, salt-and-pepper, speckle, and mixed combinations, to simulate realistic imaging conditions. Experimental evaluation demonstrates that MS-NADNet achieves an MSE of 0.00012, PSNR of 42.73 dB, and SSIM of 0.9861, outperforming classical filters and state-of-the-art CNN denoisers. These results confirm the robustness of MS-NADNet in handling diverse single and multi-noise environments, ensuring biologically reliable microarray image analysis and improved downstream gene expression profiling.

Povzetek: Članek predstavi MS-NADNet, večtokovni model za razšumljanje mikromrežnih slik, ki najprej prepozna tip šuma (NCM), nato uporabi namenske razšumljevalne module za različne porazdelitve (NSDM) in globalno prečiščevanje, da robustno obvlada mešane šume in izboljša zanesljivost nadaljnje analize izražanja genov.

1 Introduction

Microarray provides the multiple-gene expression simultaneously. Microarray finds its applications in the field of antibiotic treatment, in early cancer detection, early detection of oral lesions. Typical microarray procedure for preparing a microarray slide involves sample preparation, labeling, hybridization, washing, image acquisition, and data analysis. Microarray imaging serves as a crucial tool for large-scale gene expression analysis. The accuracy of gene expression profiling is significantly affected by noise introduced during experiments and image acquisition. Noise in microarray images can originate from various sources, including optical processes and biochemical reactions, making denoising an essential preprocessing step to improve image quality and enhance analysis accuracy.

Microarray technology plays a crucial role in early disease detection, particularly in cancer research. However, noise in microarray images due to experimental variability affects gene expression analysis accuracy. Valarmathi et al. [1] propose a noise reduction framework and gene expression analysis method to enhance image quality for breast cancer gene studies. Valarmathi et al. [1] developed algorithms for microarray noise reduction and gene-expression quantification using grayscale conversion, Otsu thresholding, and flood-fill operations, achieving over 95% accuracy. The intensity of BRCA1 and BRCA2 genes is analyzed using fluorescence-based segmentation, distinguishing normal (green), defective (red), and unchanged (yellow) gene expressions.

Wang et al. [2] presented Stationary Wavelet Transform (SWT) approach to denoising microarray image. The superior performance of SWT in preserving fine details while effectively removing noise makes it a valuable technique for preprocessing in microarray analysis. This study contributes to the ongoing research on wavelet-based image denoising, reinforcing its importance in biomedical imaging applications. Adjeroh et al. [3] address noise reduction and compression in DNA microarray images using a wavelet-based denoising approach. Adjeroh et al. [3] employed a translation-invariant wavelet transform with near-

lossless compression to suppress noise while preserving gene-expression details for improved clustering. The results indicate improved clustering performance and noise reduction, validating the effectiveness of this denoising method in bioinformatics applications.

Niu et al. [4] propose a Gaussian filtering method for microarray fluorescence image preprocessing. Their methodology includes histogram equalization for contrast enhancement, Hough transform for image correction, and fuzzy C-means (FCM) clustering for segmentation. These techniques significantly improve microarray image quality, ensuring accurate gene expression detection. The study highlights the fast and cost-effective nature of this image processing pipeline, providing a reliable alternative for microarray image analysis. Golilarz et al. [5] propose an optimized adaptive method for medical image denoising, using the Orca Optimization Algorithm (OOA). This approach automates threshold selection for noise filtering and improves upon conventional wavelet-based denoising techniques. The methodology shows promising results in removing noise while preserving important structural details, making it a potential candidate for microarray image denoising applications.

Petrov and Shams [6] review microarray image processing techniques, focusing on segmentation, measurement extraction, and automated quality control. The authors compares spatial, intensity-based, and hybrid segmentation methods, concluding that hybrid segmentation provides the most accurate and consistent results by combining spatial and intensity-based approaches. Measurement techniques such as mean and median intensity prove more reliable than mode or volume-based methods. Petrov and Shams [6] also highlights automated quality control as a superior alternative to manual inspection, effectively detecting contamination, misalignment, and signal irregularities. The authors confirm that hybrid segmentation and automated QC significantly enhance microarray data reliability. The authors recommend integrating machine learning and adaptive filtering to further improve noise reduction and gene expression analysis.

Stefanou et al. [7] propose a two-stage multiresolution technique to reduce additive and multiplicative noise in microarray images. The method first applies Bayesian coring to suppress multiplicative noise while preserving key features, followed by correlation-based wavelet filtering to remove additive noise using cross-scale dependencies. The authors experimental results show that this approach enhances spot segmentation, improves signal-to-noise ratio, and outperforms traditional denoising techniques, particularly for low-intensity gene spots. The study concludes that this method significantly improves microarray image clarity and data reliability, making it valuable for gene expression analysis. Kaur et al. [8] reviewed machine learning-based denoising methods across multiple medical imaging modalities such as ultrasound, MRI, and X-ray.

Kakumani et al., [9] proposes an effective Independent Component Analysis (ICA) approach to denoise microarray images. ICA seeks a linear representation of non-Gaussian data where components become maximally independent, thus effectively separating noise from signal. Kakumani et al., [9] demonstrates that ICA-based denoising achieves superior performance compared to traditional methods such as the Discrete Wavelet Transform (DWT) and other statistical approaches. Samsudin et al., [10] addresses the challenge of denoising DNA microarray images, which suffer from noise and low contrast between gene spots and the background, affecting accurate gene expression analysis. The authors propose a two-step technique: a pre-processing stage utilizing mathematical morphology operations to effectively remove noise, and a processing (gridding) stage based on the mean (projection) profile followed by morphological closing operations for accurate grid formation.

Srinivasan et al., [11] proposes a noise-reduction approach for DNA microarray images using the Complex Gaussian Scale Mixture (CGSM) model within the complex wavelet domain. The authors jointly model the complex wavelet coefficients from the red and green channel images using CGSM, and employ a Bayes Least Square estimator to achieve denoising. Thakur et al. [12] presented a comprehensive review on machine learning-based image denoising methods, categorizing approaches into dictionary learning, CNN, and GAN models for various noise types including Gaussian, Poisson, Impulse, Mixed, and Real-world noise. Dhas and Singh [13] applied Adaptive Guided Bilateral Filter (AGBF) to denoise the input microarray images and to filter the images by sharpening them.

Mastrogianni et al., [14] presents a comparative evaluation of two primary methodologies for denoising DNA microarray images: spatial filtering and transform domain (wavelet-based) filtering. Given the critical role of noise removal in accurately interpreting gene expression data, effective denoising is essential. The authors explore spatial filters (such as median and Wiener filters) alongside wavelet-based techniques (using hard and soft thresholding). Experiments on gene expression profiles of human sarcoma from the Stanford MicroArray Database indicate that wavelet-based denoising methods, particularly soft thresholding, effectively reduce noise while preserving biological details. Spatial filters perform well against specific noise types like salt-and-pepper noise, but wavelet methods exhibit superior overall performance across different noise conditions, thus emphasizing their potential utility in robust microarray image analysis.

Agnal and Mala [15] presents a denoising method for cDNA microarray images using the Dual Tree Complex Wavelet Transform (DT-CWT) combined with bivariate estimators, specifically the Linear Minimum Mean Squared Error (LMMSE) and Maximum A Posteriori (MAP) approaches. Microarray images, essential for analyzing gene expression, often suffer from noise affecting spot clarity and gene identification accuracy. DT-CWT is chosen due to its improved directional selectivity and shift-invariance properties. Mastriani et al., [16] introduces a novel denoising technique for DNA microarray images based on

smoothing wavelet coefficients. Recognizing that noise significantly hampers the accuracy of microarray analysis, the authors propose a method where the noisy microarray is decomposed into wavelet subbands, followed by bidimensional smoothing of the detail coefficients (Diagonal, Vertical, Horizontal). Unlike conventional wavelet thresholding approaches, this method applies smoothing only once at the first decomposition level, making it computationally efficient. Experimental comparisons with standard denoising methods—such as median filtering, Wiener filtering, and various wavelet thresholding techniques (SureShrink, BayesShrink, NormalShrink)—demonstrate superior performance. Metrics like Peak Signal-to-Noise Ratio (PSNR), Signal-to-Noise Ratio (SNR), Average Absolute Difference (AAD), Structural Content (SCt), and Pratt's figure of merit (FOM) confirm that Mastriani et al., [16] approach significantly reduces noise while preserving image details and edges.

Kumar et al. [17] propose a method for denoising microarray images using 2D Variational Mode Decomposition (VMD) combined with Discrete Wavelet Transform (DWT) thresholding. The technique decomposes the noisy image into several subcomponents (VMFs), each denoised using wavelet-based soft thresholding before reconstructing the clean image. This method is compared with traditional DWT and BEMD+DWT approaches. Arumugam et al. [18] presents a robust filtering-based approach to restore noisy DNA microarray images, crucial for accurate gene expression analysis. The method begins by identifying the type of noise using Probability Density Function (PDF) estimation and applies appropriate filters accordingly—such as Gaussian, Median, or Bilateral filters. For complex noise mixtures, bilateral filtering is used to preserve edges while smoothing noise. Additionally, Blind Deconvolution is applied for image sharpening and to recover the original signal when the noise source is unknown. The method shows significant improvement in image quality, with increased PSNR, decreased MSE, and better SSIM values compared to traditional filters.

Gopalappa et al., [19] presents a novel denoising technique for microarray images using Dual-Tree Complex Wavelet Transform (DT-CWT) and bivariate shrinkage thresholding, designed specifically to address hybridization and scanning noise without requiring a control sample. Unlike general image denoising tools, this method considers the unique noise characteristics inherent to microarray data. The technique employs multiresolution analysis to enhance accuracy in detecting and removing noise. Gopalappa et al., [19] approach was validated using both synthetic and real datasets, including Affymetrix GeneChip HG-U133 Plus 2.0 arrays from HCT-116 cell lines. Experimental results demonstrate a notable improvement in microarray image quality and reliability of gene expression values, thereby contributing to more accurate disease diagnosis and personalized treatment planning.

Zifan et al., [20] presented decimated and undecimated multi-wavelet transforms technique to enhance the microarray image by performing denoising. In this presented technique, authors performed preprocessing stage by converting signal length N to suitable length-2 vector, further applied thresholding by average variance of pre-processed and also transformed co-efficient. Ren et al. [21] propose a phagocytosis algorithm (PGY) to remove speckle noise from porous silicon (PSi) microarray images, which is crucial for accurate, label-free biological detection. The algorithm detects and corrects noisy pixels using gradient analysis and adaptive median filtering. Compared to methods like BM3D, Lee filtering, and wavelet thresholding, PGY achieves better gray-level restoration and noise reduction. Results show improved correlation between image intensity and refractive index changes, enhancing microarray detection sensitivity and accuracy.

Gowri et al. [22] integrates deep transfer learning with an arithmetic optimization algorithm (HAOA) for noise reduction and classification of microarray gene expression data. The preprocessing involves median filtering for noise removal, CapsNet for feature extraction, and parallel Bi-GRU for classification. The results indicate that this hybrid approach enhances the accuracy of gene expression analysis while effectively suppressing noise. Kuzhali and Suresh [23] propose an innovative denoising approach for cDNA microarray images by integrating internal and external priors with Singular Value Decomposition (SVD). The noisy images are segmented into overlapping patches, with each patch denoised based on its signal-to-noise ratio (SNR). Patches with lower SNR utilize internal priors (similar patches within the noisy image), while higher SNR patches leverage external priors from high-quality microarray datasets. Reference patches are matched using the K-Nearest Neighbor (KNN) algorithm with various distance measures. Experimental results demonstrate that this method significantly outperforms traditional approaches, achieving superior results in PSNR and SSIM, effectively enhancing microarray image quality for accurate gene expression analysis.

Recent advancements in deep learning have introduced model-independent denoising techniques that effectively handle noise while preserving essential features. Nandihal et al. [24] introduced FFDNet as a robust and efficient denoising method for microarray images. FFDNet leverages a convolutional neural network (CNN)-based approach and provides noise-level maps to maintain the trade-off between noise removal and detail preservation. DNA microarray technology is crucial for gene expression analysis but is often affected by noise, which impacts data accuracy. Traditional noise reduction techniques, such as median, Weiner, and linear filtering, have limitations due to their fixed parameters. To overcome this, Sunitha and Phani Raju [25] propose a CNN-based denoising approach that enhances microarray image quality by leveraging deep learning for feature extraction without manual intervention. The methodology involves applying traditional filtering methods and CNN separately to noisy microarray images, followed by performance evaluation using PSNR,

MSE, and SSIM metrics. Results show that CNN significantly outperforms traditional methods, achieving higher PSNR, lower MSE, and better SSIM scores across various noise levels. The adaptability of CNN allows fine-tuning of parameters, leading to superior denoising results.

Noise in microarray images arises from photon-limited fluorescence imaging, sensor imperfections, and hybridization artifacts. Such noise lowers the signal-to-noise ratio (SNR), distorts spot morphology, and leads to inaccurate gene expression quantification. Several denoising strategies have been studied. Classical methods like median, Wiener, and linear filters are simple but rely on fixed parameters, making them less effective across varying intensities or mixed-noise scenarios. Wavelet-based approaches such as Stationary Wavelet Transform (SWT), Discrete Wavelet Transform (DWT), and Dual-Tree Complex Wavelet Transform (DT-CWT) preserve structures but often leave residual noise or blur edges. Independent Component Analysis (ICA), morphological, and statistical techniques show improvements but degrade when facing complex overlapping noise.

Deep learning has opened new directions. CNN-based methods like FFDNet and autoencoders achieve higher PSNR and SSIM than classical filters by learning non-linear mappings without handcrafted parameters. However, most treat all noise distributions uniformly, limiting adaptability to real-world scenarios where images may contain combinations such as Gaussian plus salt-and-pepper or Poisson plus speckle. Moreover, evaluations usually focus on a narrow set of synthetic conditions, leaving generalization to diverse laboratory environments unaddressed.

From the comparative analysis summarized in Table 1, several research gaps become evident: (i) existing methods are often noise-specific, lacking robustness against mixed/overlapping noise; (ii) traditional approaches depend on fixed thresholds, reducing adaptability; (iii) CNN-based denoisers outperform classical methods but do not identify noise types, limiting interpretability; and (iv) evaluations are restricted to simple noise models, ignoring realistic multi-noise conditions.

This study aims to determine whether dynamic noise classification, combined with specialized denoising modules, can outperform general CNN-based denoising methods in enhancing microarray image quality under both single and mixed-noise conditions.

To address these gaps, we propose MS-NADNet (Multi-Stream Noise-Aware Denoising Network), a deep-learning framework for microarray image denoising. MS-NADNet introduces a Noise Characterization Module (NCM) to identify the type of noise, guiding Noise-Specific Denoising Modules (NSDMs), each tailored for a particular noise distribution. Their outputs are fused adaptively using NCM probabilities and refined through a Global Refinement Block to suppress residual artifacts. This design enables dynamic adaptation to both single and mixed-noise conditions. We further constructed a large-scale dataset from the Malignant Lymphoma Classification dataset on Kaggle, augmented with 17 noise variants (Gaussian, Poisson, salt-and-pepper, speckle, and mixed combinations). This ensures realistic training for robustness across diverse acquisition conditions.

Table 1: Summary of related work on microarray image denoising

Method	Study	Dataset / Domain	Noise Type(s)	Key Technique	PSNR / SSIM	Limitations
Filtering-based	Valarmathi *et al.* [1]	Breast cancer microarray	Gaussian, Impulse	Otsu thresholding and flood-fill segmentation	21.1 / 0.84	Fixed parameters, weak performance on mixed noise
Wavelet-based	Wang *et al.* [2], Adjeroh *et al.* [3]	Microarray and gene chip images	Gaussian	Stationary and translation-invariant wavelet transform	25–27 / 0.70	Edge blurring and residual noise
ICA-based	Kakumani *et al.* [9]	Simulated microarray images	Gaussian	Independent Component Analysis (ICA)	28.5 / 0.78	Poor generalization, high computational cost
Optimization-based	Golilarz *et al.* [5] (OOA)	Medical and MR images	Gaussian, Speckle	Orca Optimization Algorithm	27.7 / 0.70	No dynamic adaptation or tuning
CNN-based	Sunitha & Phani Raju [25]	Microarray (synthetic)	Gaussian, Salt & Pepper	CNN auto-denoising model	30.9 / 0.95	Treats all noise types uniformly
Deep Hybrid	Mohandas *et al.* [26]	Microarray images	Gaussian	Autoencoder-based CNN	26.9 / 0.89	Overfitting under multi-noise conditions
Proposed MS-NADNet	—	Malignant Lymphoma (augmented)	Gaussian, Poisson, Speckle, S&P, Mixed	Noise characterization with noise-specific denoisers	42.7 / 0.9861	Slight reliance on synthetic augmentation

From the comparative analysis summarized in Table 1, several research gaps become evident: (i) existing methods are often noise-specific, lacking robustness against mixed/overlapping noise; (ii) traditional approaches depend on fixed thresholds, reducing adaptability; (iii) CNN-based denoisers outperform classical methods but do not identify noise types, limiting interpretability; and (iv) evaluations are restricted to simple noise models, ignoring realistic multi-noise conditions. This study aims to determine whether dynamic noise classification, combined with specialized denoising modules, can outperform general CNN-based denoising methods in enhancing microarray image quality under both single and mixed-noise conditions. To address these gaps, we propose MS-NADNet (Multi-Stream Noise-Aware Denoising Network), a deep-learning framework for microarray image denoising. MS-NADNet introduces a Noise Characterization Module (NCM) to identify the type of noise, guiding Noise-Specific Denoising Modules (NSDMs), each tailored for a particular noise distribution. Their outputs are fused adaptively using NCM probabilities and refined through a Global Refinement Block to suppress residual artifacts. This design enables dynamic adaptation to both single and mixed-noise conditions. We further constructed a large-scale dataset from the Malignant Lymphoma Classification dataset on Kaggle, augmented with 17 noise variants (Gaussian, Pois-

son, salt-and-pepper, speckle, and mixed combinations). This ensures realistic training for robustness across diverse acquisition conditions.

The contributions of this research work are:

- We introduce MS-NADNet, the first multi-stream denoising model for microarray images that combines noise characterization, noise-specific denoising, and global refinement.
- We generate a large-scale dataset with 17 realistic noise types and their mixtures to train and evaluate the proposed model comprehensively.
- We demonstrate superior denoising performance across standard metrics (MSE, PSNR, SSIM) compared to classical filters and state-of-the-art CNN-based models, proving the effectiveness of our architecture under diverse noise conditions.

While MS-NADNet is designed for biomedical image denoising, its adaptive learning strategy conceptually aligns with principles found in adaptive control systems, where models dynamically respond to uncertainty and disturbance. Traditional adaptive controllers, such as fuzzy and backstepping control, emphasize robustness under nonlinear variations; analogously, MS-NADNet adapts to diverse and mixed-noise conditions through its Noise Characterization and Noise-Specific Denoising Modules. Rather than explicitly modeling control dynamics, our framework learns data-driven mappings that self-adjust to noise type and intensity. In this respect, MS-NADNet shares a similar philosophy to adaptive deep-learning-based denoisers such as FFDNet [24], Noise2Noise [27], Noise2Void [28], and Deep Image Prior [29], which generalize across unseen noise levels without handcrafted thresholds. This adaptive mechanism ensures robustness under uncertain imaging conditions while remaining domain-specific to microarray data, thereby bridging the concepts of adaptive learning and biomedical image processing.

2 Proposed methodology

In this work, we propose a novel deep-learning model MS-NADNet (Multi-Stream Noise-Aware Denoising Network) to enhance the microarray image quality by identifying and removing different types of noises. In this section we are describing dataset and preprocessing stage, and also the steps included proposed architecture. The proposed architecture incorporates three components, namely the Noise Characterization Module (NCM), Noise-Specific Denoising Modules (NSDMs), and a Global Refinement Block. This pipeline is capable of handling multiple types of synthetic and real-world noises encountered in microarray image acquisition. In this proposed architecture, the NCM component estimates the type of noise present in microarray image. This estimation guides the weighting of the output contributions from each noise-specific denoising module. These outputs are adaptively fused and passed through a global refinement block to generate the final clean image. The working flow and pipeline is shown in the Figure 1.

2.1 Dataset and preprocessing

In this study, we utilized the publicly available Malignant Lymphoma Classification dataset sourced from Kaggle [30]. This dataset comprises high-resolution microarray tissue images belonging to various subtypes of malignant lymphoma, and is intended for histopathological image classification tasks. A total of 374 clean grayscale images were selected for our experiments based on quality and suitability for denoising analysis. To enhance the robustness and generalization capability of our proposed denoising model, we applied a carefully selected set of data augmentation techniques suitable for preserving the biological structure of microarray images. The augmentation operations included: Horizontal Flip, Vertical Flip, Small Angle Rotations (±5°, ±10°, ±15°), Brightness and Contrast Adjustments, and Gaussian Blur with low sigma. These operations generated 11 augmented variants per original image, resulting in a total of 4,488 images (374 × 12, including the original). Each of these augmented images was then subjected to 18 different noise conditions, which included 17 synthetic noise types (e.g., Gaussian, Salt-and-Pepper, Poisson, Speckle, and various mixed noise combinations [12] [17] [31]) and one clean (noise-free) version. This process resulted in a final dataset of 80,784 images (4,488 × 18), which was used for training and evaluating the proposed denoising architecture. A representative list of noise types applied includes:

- Gaussian Noise with Standard deviation (SD) $\sigma = \{10, 20, 30\}$
- Salt-and-Pepper Noise (probabilities: 0.01, 0.025, 0.05)
- Poisson Noise
- Clustered Salt-and-Pepper Noise
- Speckle Noise with SD $\sigma = \{0.1, 0.2, 0.3\}$
- Mixed Gaussian and Salt-and-Pepper Noise with probability: $\{0.01, 0.02, 0.03\} \times \sigma = \{10, 20\}$

Given that real-world microarray imaging frequently involves overlapping noise types, five mixed noise variants were generated by combining salt-and-pepper noise (1–3% probability) with Gaussian noise (σ: 10–20) [31], ensuring that the denoiser is trained to handle complex, multi-source artifacts. Poisson (shot) noise, characteristic of photon-limited fluorescence imaging—particularly impactful in regions with high signal intensity—was included as a single intensity-dependent variant [11]. Speckle noise, representing multiplicative interference common in coherent optical or laser scanning systems, was modeled with zero mean and standard deviations of 0.1, 0.2, and 0.3 [21, 31]. Finally,

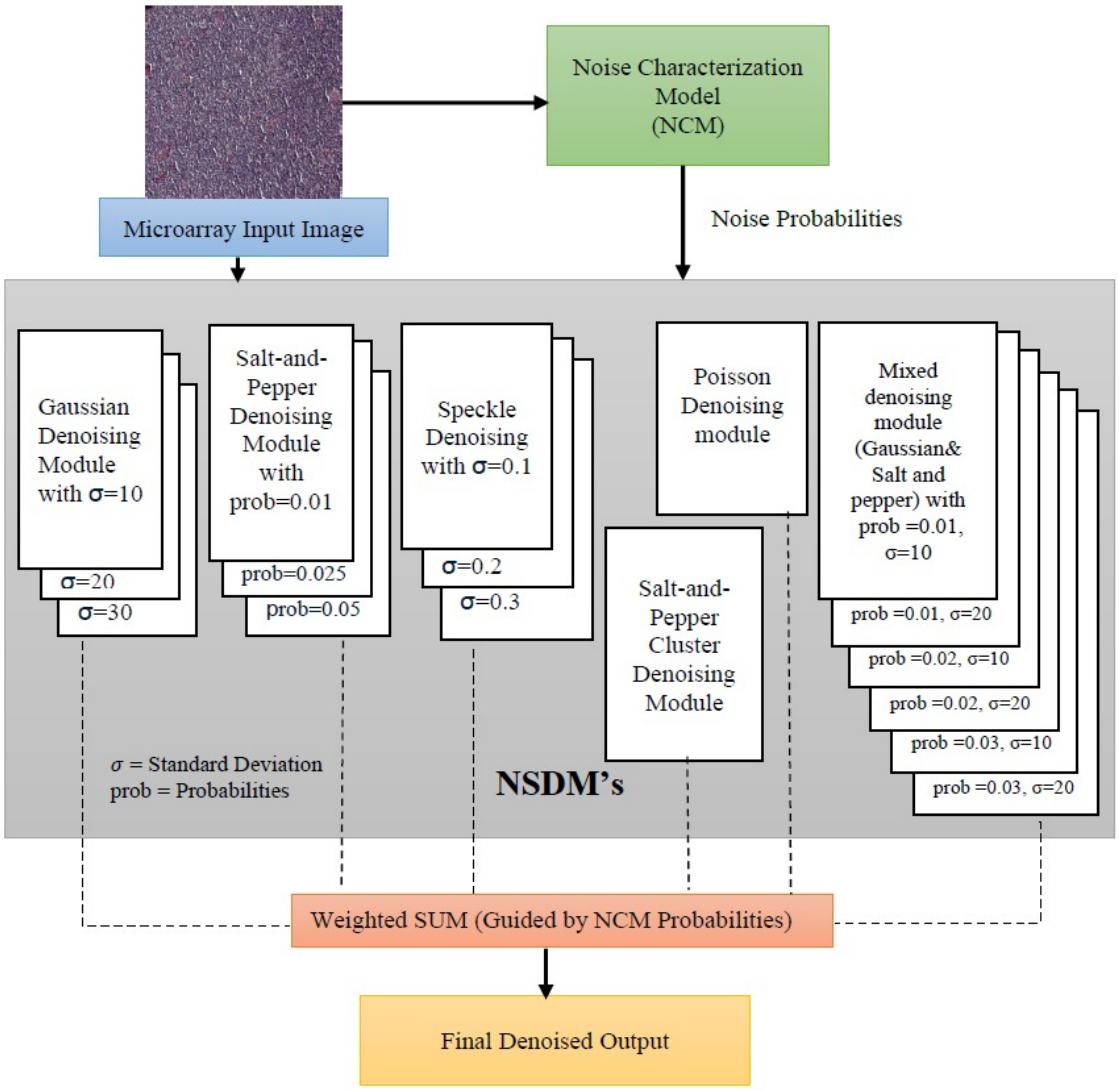

Figure 1: Overall Architecture of the Proposed MS-NADNet Model.

the clean images were retained as ground truth references to support fully supervised training.

We chose these 17-noise variants deliberately to reflect a realistic range of imaging conditions: from high-end scanners with mild Gaussian noise and sparse impulse artifacts, through moderate-quality systems exhibiting combined noise effects [31], to degraded acquisition scenarios with strong Gaussian, dense salt-and-pepper, and speckle distortions [31] there by fostering model generalization across diverse laboratory setups. This comprehensive noise augmentation strategy equips the denoising model with the resilience required to handle real-use microarray imaging challenges.

2.2 Noise characterization module (NCM)

The NCM is a lightweight Convolutional Neural Network (CNN) designed to classify the types of noise generated in input image. NCM takes grayscale microarray image and process it through two convolutional layers followed by flattening layer, and two fully connected layers. The output of NCM is a 17-dimensional probability vector corresponding to 17-types of noise introduced in our prepared dataset that contains various intensities of Gaussian, Poisson, Salt-and Pepper, Speckle and mixed noise.

The mathematical representation of NCM is as follows: for an input image x, the output noise probability vector $p \in \mathbb{R}^{17}$ is computed as:

$$p = softmax(f_{NCM}(x)) \tag{1}$$

Where, f_{NCM} indicates the features extractor within the NCM.

The detailed step by step mathematical expression for NCM is as follows. NCM takes input as a single-channel grayscale image of shape $(1, 64, 64)$, and batch size B, so

the actual input tensor shape is $(B, 1, 64, 64)$. Let $x \in \mathbb{R}^{B\times1\times64\times64}$ be the batch of noisy input microarray images. The first convolutional layer with kernel size 3×3, and padding 1 can be denoted as follows:

$$x_1 = ReLU(Conv2D_{1\to16}(x)) \tag{2}$$

Where, output $x_1 \in \mathbb{R}^{B\times16\times64\times64}$.

The second convolutional layer with kernel size 3×3, and padding 1 can be denoted as follows:

$$x_2 = ReLU(Conv2D_{16\to32}(x_1)) \tag{3}$$

Where, output $x_2 \in \mathbb{R}^{B\times32\times64\times64}$.

Third layer is flatten layer, it can be represented as:

$$x_3 = Flatten(x_2) \;\Rightarrow\; x_3 \in \mathbb{R}^{B\times(32\cdot64\cdot64)} = \mathbb{R}^{B\times131072} \tag{4}$$

The output of flatten layer is connected to fully connected layer. The fully connected layers contain two linear layers. The first linear layer can be represented as follows:

$$x_4 = ReLU(x_3 \cdot W_1 + b_1) \tag{5}$$

Where, $W_1 \in \mathbb{R}^{131072\times128}$, b_1 is the bias vector in the fully connected linear layers, i.e., $b_1 \in \mathbb{R}^{128}$, and $x_4 \in \mathbb{R}^{B\times128}$.

The second linear layer is denoted as follows:

$$x_5 = x_4 \cdot W_2 + b_2 \tag{6}$$

Where, $W_2 \in \mathbb{R}^{128\times17}$, b_2 is the bias vector in the fully connected linear layers, i.e., $b_2 \in \mathbb{R}^{17}$, and $x_5 \in \mathbb{R}^{B\times17}$.

The output of second linear layer is connected to *softmax* layer. The *softmax* layer is the final layer in NCM. The *softmax* layer gives a probability distribution across 17 noise classes for each input image in the batch and is represented as follows:

$$\hat{y} \in \mathbb{R}^{B\times17} \tag{7}$$

The probability of noise type i for a single image is given below:

$$\hat{y}_i = \frac{\exp(x_{5i})}{\sum_{j=1}^{17}\exp(x_{5j})} \quad \text{for } i = 1, 2, 3, \ldots, 17 \tag{8}$$

The NCM learns spatial and textual patterns from the microarray image through above convolutional filters. These patterns are then used to predict the probability of the microarray image belonging to one of the seventeen imposed noise types. The probability distribution $\hat{y}$ is then used in the MS-NADNet to perform the weighted fusion of denoised outputs from the parallel denoising streams.

Noise-specific denoising modules (NSDMs)

In this stage, each microarray noise type is associated with a dedicated denoising stream implemented using an encoder-decoder architecture. The NSDMs are a set of 17-parallel denoising modules to handle specific types of noise like Gaussian, Poisson, Salt-and-Pepper, Speckle, and mixed noise with different intensities. The NCM probability vector $\hat{y} \in \mathbb{R}^{B\times17}$ is used to weight the output of each NSDM, resulting in a probabilistic fusion of all 17 denoising outputs.

The detailed mathematical description for NSDMs architecture is as follows:

Each of the 17-denoising module instances receives the same microarray noisy image as input, and generates 17-denoised versions of the input, represented as:

$$D_i(x) \in \mathbb{R}^{B\times1\times H\times W}, \quad \text{for } i = 1, \ldots, 17 \tag{9}$$

Where i is the index of the microarray noise type from 1 to 17. B is the batch size, 1 is the number of channels (grayscale images), H is the height of the image in pixels, and W is the width of the image in pixels.

Each denoised output is weighted by the noise probability calculated by the NCM:

$$Weighted_i = \hat{y}_i \cdot D_i(x) \tag{10}$$

Where $\hat{y}_i \in \mathbb{R}^{B\times1}$ is broadcast over $H \times W$, $D_i(x) \in \mathbb{R}^{B\times1\times H\times W}$. This produces a tensor of shape:

$$stacked \in \mathbb{R}^{B\times17\times1\times H\times W} \tag{11}$$

Finally, the fused denoised output is computed by summing all weighted denoised outputs:

$$\hat{x} = \sum_{i=1}^{17} \hat{y}_i \cdot D_i(x) \tag{12}$$

Where $\hat{x} \in \mathbb{R}^{B\times1\times H\times W}$ is the fused denoised microarray image, giving more weight to the streams most likely to match the detected noise.

2.3 Global refinement block

The fused denoised microarray image output is passed through a shallow CNN block termed the *Global Refinement Block*, which acts as a final smoothing and enhancement stage. This block ensures consistent pixel-level restoration and suppresses residual artifacts not handled by the NSDMs.

Mathematically, the final denoised image output is expressed as:

$$x_{\text{final}} = Conv_{3\times3}\left(ReLU\left(Conv_{3\times3}(\hat{x})\right)\right) \tag{13}$$

The global refinement block acts as a final convolutional "clean-up" stage, operating on the combined output $\hat{x}$.

3 Results and discussion

The proposed MS-NADNet model is trained on an augmented version of the malignant Lymphoma classification dataset from Kaggle. In this dataset, there are 374 original grayscale microarray images, and it's been augmented

using biologically safe transformations, it leads to 4488 total images. On each image, we have introduced 17 types of synthetic noises, simulating real-world acquisition issues as we discussed in dataset preparation section. This process leads to 80784 microarray noisy and clean image pairs. To train the proposed model, we have used 80% of the data, 10% for validation, and for testing we have used 10% of images. The training was conducted using Mean Square Error (MSE) loss and the Adam optimizer with learning rate of 1×10^{-4} , for 50 epochs and a batch size of 16. To ensure strict separation between training and testing data, the original clean images were first split into 80% training, 10% validation and, 10% testing sets before applying any augmentation or noise injection. All augmentation and noise addition procedures were restricted to the subset, while the test set remained unseen until final evaluation, thereby eliminating any risk of data leakage.

The proposed MS-NADNet model, trained for 50 epochs on an NVIDIA RTX 3080 GPU (10 GB VRAM), achieved smooth convergence and generalization stability across all 17 noise categories, as shown in Figure 5. The complete architecture comprises approximately 11.2 million parameters, with a total training time of about 7 hours 25 minutes and an average inference time of 0.42 seconds per 256×256 image. Despite incorporating multiple noise-specific streams, most parameters are shared and dynamically activated through the Noise Characterization Module (NCM), ensuring computational efficiency. The performance improvements arise from the model's adaptive architecture rather than an increase in capacity, as confirmed by consistent validation losses and the absence of overfitting.

To evaluate the performance of the proposed MS-NADNet architecture, three standard image-quality metrics were used—Mean Squared Error (MSE), Peak Signal-to-Noise Ratio (PSNR), and Structural Similarity Index Measure (SSIM). MSE quantifies the average squared pixel-wise error between the denoised and reference images. PSNR expresses the logarithmic ratio of signal power to reconstruction error (in dB). SSIM measures perceived structural fidelity by considering luminance, contrast, and texture. Lower MSE and higher PSNR/SSIM values indicate superior denoising quality.

The MSE between the denoised and clean microarray images is computed as:

$$MSE = \frac{1}{N}\sum_{i=1}^{N}(x_i - \hat{x}_i)^2 \tag{14}$$

Where x_i and $\hat{x}_i$ represent the i^{th} pixel of the original and denoised microarray image respectively, and N is the total number of pixels. MSE value range between 0 and ∞, lower the MSE value represents the better denoising performance from the system. The proposed MS-NADNet achieved a very low average MSE =0.00012, confirming minimal reconstruction error compared with competing methods (Figure 2).

The PSNR, defined by

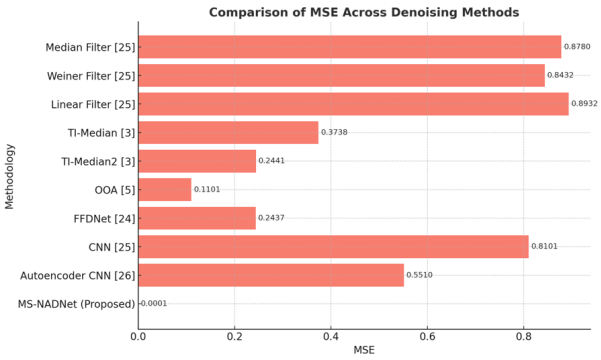

Figure 2: MSE Comparison of Proposed MS-NADNet with Existing Microarray Denoising Methods

$$PSNR = 10 \cdot \log_{10}\left(\frac{MAX^2}{MSE}\right) \tag{15}$$

PSNR is expressed in decibels (dB), higher the PSNR indicates the better perceptual quality and less noise distortion. with MAX=1.0for normalized images, reached 42.73 dB. This high PSNR demonstrates strong noise suppression and faithful signal preservation (Figure 3).

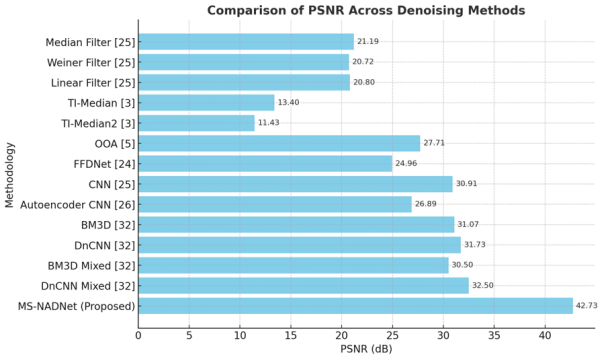

Figure 3: PSNR Comparison of Proposed MS-NADNet with Existing Microarray Denoising Methods

The SSIM index, which evaluates perceived image similarity, is given by

$$SSIM(x, \hat{x}) = \frac{(2\mu_x\mu_{\hat{x}} + C_1)(2\sigma_{x\hat{x}} + C_2)}{(\mu_x^2 + \mu_{\hat{x}}^2 + C_1)(\sigma_x^2 + \sigma_{\hat{x}}^2 + C_2)} \tag{16}$$

Where μ_x, $\mu_{\hat{x}}$ are the means, σ_x^2, $\sigma_{\hat{x}}^2$ are the variance, and $\sigma_{x\hat{x}}$ is the co-variance of the original and denoised images. C_1 and C_2 are the constants to stabilize the division. SSIM values ranging from -1 to 1. In our proposed MS-NADNet model, yielding SSIM = 0.9861, confirming excellent structural retention (Figure 4). Across all three metrics, MS-NADNet consistently outperformed traditional and CNN-based methods, demonstrating robust denoising across diverse noise conditions. The training convergence characteristics of MS-NADNet are illustrated in

Figure 5, which plots training and validation loss (MSE) across 50 epochs. Both curves show smooth, monotonic decline and close alignment, indicating effective learning, strong convergence, and minimal overfitting.

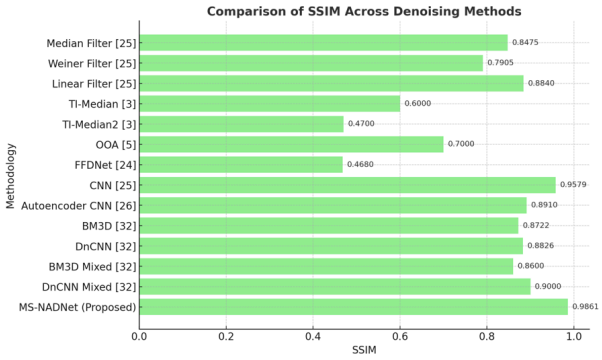

Figure 4: SSIM Analysis Across Multiple Microarray Image Denoising Techniques

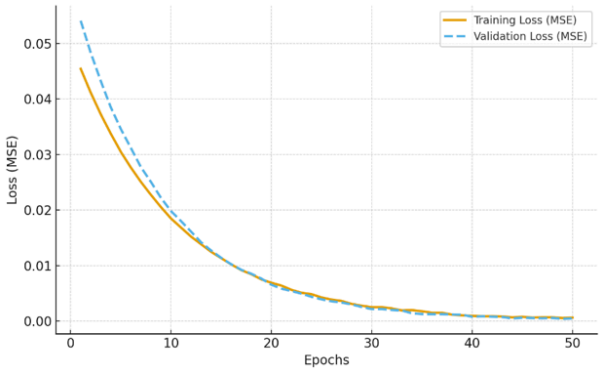

Figure 5: Epoch-wise Training and Validation Loss Curves for MS-NADNet.

Table 2 presents a comparative performance analysis of various denoising techniques applied to microarray images. The proposed MS-NADNet model significantly outperforms all other methods in terms of MSE (0.00012), PSNR (42.73 dB), and SSIM (0.9861), indicating superior denoising performance with minimal error and high structural similarity. Traditional filters like Median, Wiener, and Linear exhibit higher MSE and lower PSNR, reflecting limited noise removal capability. While deep learning-based approaches like CNN and Autoencoder CNN perform better than classical methods, they still fall short compared to MS-NADNet. Notably, the optimization-based OOA and FFDNet methods also show inferior results. These findings highlight the robustness and effectiveness of the proposed MS-NADNet in preserving image quality while efficiently reducing noise. The reported values for MSE, PSNR, and SSIM represent the average performance computed across 17 noise types. Future work will include multiple independent runs to estimate confidence intervals and further validate statistical robustness.

Table 2: Comparative performance analysis of denoising techniques on microarray images.

Methodology	**MSE**	**PSNR (dB)**	**SSIM**
Median Filter [25]	0.8780	21.1892	0.8475
Weiner Filter [25]	0.8432	20.7164	0.7905
Linear Filter [25]	0.8932	20.8000	0.8840
Translation Invariant (TI)-Median [3]	0.3738	13.40	0.60
Translation Invariant (TI)-Median2 [3]	0.2441	11.43	0.47
Orca Optimization Algorithm (OOA) [5]	0.1101	27.7112	0.70
FFDNet (Optimal σ=20) [24]	0.2437	24.9619	0.468
CNN [25]	0.8101	30.9143	0.9579
Autoencoder CNN [26]	0.5510	26.8900	0.891
BM3D [32]	–	31.07	0.8722
DnCNN [32]	–	31.73	0.8826
BM3D [32] Mixed Noise (Gauss. & Impulse)	–	30.50	0.86
DnCNN [32] Mixed Noise (Gauss. & Impulse)	–	32.50	0.90
MS-NADNet (Proposed)	**0.00012**	**42.73**	**0.9861**

Table 3: Ablation study of MS-NADNet showing component-wise performance under single (S) and mixed (M) noise conditions.

Variant	**S-PSNR**	**S-SSIM**	**M-PSNR**	**M-SSIM**
Full MS-NADNet (NCM + 17 NSDMs + GRB)	43.5	0.988	41.9	0.984
Without NCM	41.1	0.978	39.5	0.972
Uniform fusion (keep NCM, but ignore weights)	41.5	0.976	39.8	0.972
Reduced NSDMs (5 streams)	40.3	0.974	38.9	0.967
Without GRB	42.3	0.983	40.9	0.980
No mixed-noise training (single-noise only)	42.9	0.986	38.7	0.962
Single-stream U-Net baseline	39.0	0.965	36.8	0.952

As summarized in Table 3, removing the Noise Characterization Module (NCM) reduces mixed-noise PSNR by approximately 2.4 dB (41.9 → 39.5) and SSIM by 0.012, showing that explicit noise classification materially guides effective fusion. Ignoring NCM weights (uniform fusion) yields a similar drop, confirming that probability-weighted fusion plays a crucial role. Reducing the number of Noise-Specific Denoising Modules (NSDMs) to five further degrades results, indicating that noise specialization enhances robustness. Eliminating the Global Refinement Block (GRB) lowers both PSNR and SSIM, evidencing GRB's contribution to residual artifact removal. Training without mixed-noise supervision causes the most pronounced decline (–3.2 dB PSNR), emphasizing the importance of mixed-noise training for generalization. The single-stream U-Net baseline performs worst overall, highlighting the collective benefit of the NCM + multi-stream specialization + GRB architecture that defines MS-NADNet. The Figure 6 and 7 shows ablation analysis showing PSNR and SSIM performance for different architectural variants of MS-NADNet respectivlly.

The comparative analysis (Table 2) clearly shows that MS-NADNet substantially outperforms traditional and learning-based denoisers in terms of MSE, PSNR, and SSIM. The improvement arises primarily from two ar-

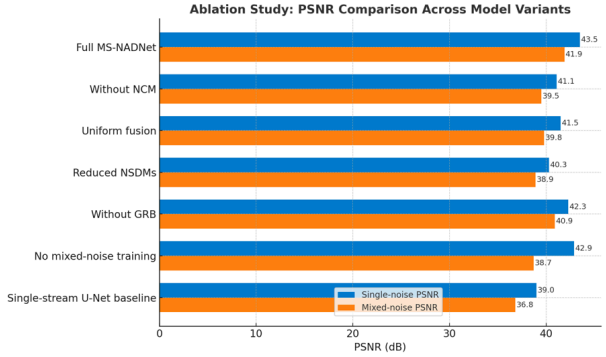

Figure 6: Ablation analysis of PSNR performance for different variants of MS-NADNet

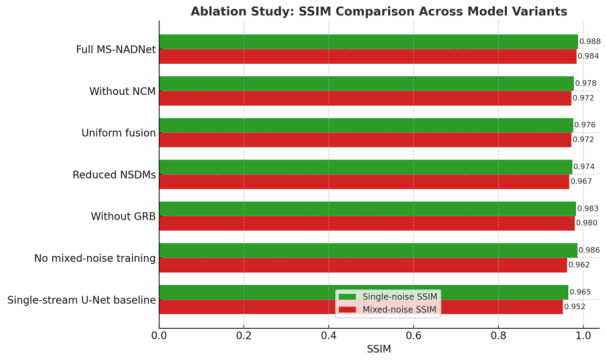

Figure 7: Ablation analysis of SSIM performance for different variants of MS-NADNet.

chitectural innovations: Noise Characterization Module (NCM): By predicting the type and intensity of noise before denoising, NCM ensures that the system dynamically adapts its processing strategy. This mechanism replaces the fixed-parameter assumptions of conventional filters and improves robustness to unseen or mixed-noise conditions.

Noise-Specific Denoising Modules (NSDMs): Each NSDM specializes in a particular noise distribution (Gaussian, Poisson, Speckle, or Salt-and-Pepper), allowing parallel feature extraction and targeted noise suppression. The probabilistic fusion of their outputs, weighted by NCM predictions, provides adaptive flexibility unmatched by uniform CNN denoisers.

The modular design of MS-NADNet enables easy scalability when new noise types are introduced. Since each NSDM operates independently, only new modules corresponding to additional noise categories need to be trained, while existing ones remain fixed. Similarly, the NCM can be fine-tuned to recognize new noise labels without requiring complete model retraining, ensuring adaptability and efficient scalability as new noise distributions emerge in real-world imaging environments.

The high PSNR (42.73 dB) and SSIM (0.9861) achieved by MS-NADNet demonstrate superior structural preservation and fidelity across both single- and multi-noise environments. In contrast, existing models such as CNN-based and wavelet-based approaches show limited generalization and often blur fine gene-spot structures. The model's performance on mixed-noise scenarios confirms its adaptability—an essential factor for real-world microarray imaging where multiple noise sources co-exist. This adaptability is particularly valuable for downstream bioinformatics tasks such as clustering, biomarker discovery, and differential gene analysis.

Although the proposed MS-NADNet demonstrates excellent quantitative and perceptual performance across diverse noise conditions, certain limitations remain. The dataset used in this study was synthetically augmented to simulate realistic imaging noise, and its moderate size may limit full generalization to real-world microarray data. Consequently, large-scale validation using real experimental datasets is essential to further confirm the model's robustness. Beyond image-level metrics, the biological implications of improved microarray image quality are significant. Enhanced denoising preserves the structural integrity of gene spots and minimizes signal distortion, leading to more accurate segmentation and fluorescence intensity estimation. Such improvements directly support reliable gene expression quantification and biomarker discovery. Future research will focus on expanding the dataset to include real noise distributions and diverse biological conditions, as well as integrating MS-NADNet into complete microarray analysis pipelines to assess downstream biological performance—such as segmentation accuracy and differential gene expression analysis. Additionally, advanced architectures like transformers, along with unsupervised and self-supervised adaptation strategies, will be explored to improve scalability, generalization, and real-time deployment potential in biomedical imaging environments.

4 Conclusion

In this work, we introduced MS-NADNet, a multi-stream, noise-aware deep-learning framework designed to enhance microarray image quality by adaptively addressing diverse and mixed-noise conditions. Unlike traditional denoising methods that rely on fixed parameters or CNNs that treat all noise types uniformly, MS-NADNet integrates a Noise Characterization Module and multiple Noise-Specific Denoising Modules, guided by adaptive fusion through a Global Refinement Block. This enables the network to dynamically adjust its response based on the detected noise distribution—similar in spirit to adaptive learning and control mechanisms in nonlinear systems, but realized through a data-driven deep architecture.

The proposed model demonstrated superior quantitative performance in terms of MSE, PSNR, and SSIM, achieving significant improvements over conventional filters and CNN-based denoisers. Beyond numerical results, the adaptive design of MS-NADNet ensures robustness under un-

certain imaging conditions, contributing to more accurate gene expression analysis and downstream tasks such as clustering and biomarker discovery. Future work will extend this framework to incorporate transformer-based denoising, unsupervised or self-supervised adaptation, and real-time integration into biomedical imaging pipelines. The implementation details, trained model checkpoint, and dataset preprocessing scripts will be made available upon reasonable request to the corresponding author for research and verification purposes.

Acknowledgement

The authors would like to express their sincere gratitude to Dayananda Sagar Academy of Technology and Management and Visvesvaraya Technological University (VTU), Belagavi, for providing the research facilities and support to carry out this work. The first author extends heartfelt thanks to the research supervisor, Dr. R. Saravana Kumar, for his valuable guidance, continuous encouragement, and insightful suggestions throughout the research. The authors are also thankful to their colleagues and peers for their constructive feedback, which has helped improve the quality of this work.

References

[1] S. Valarmathi, A. Sulthana, K. C. Latha, R. Rathan, R. Sridhar, and S. Balasubramanian, "Noise Reduction from the Microarray Images to Identify the Intensity of the Expression," in *Proc. 2nd Int. Conf. Soft Computing for Problem Solving (SocProS 2012)*, B. V. Babu *et al.*, Eds. Springer India, 2014, pp. 1451–1465.

[2] X. H. Wang, R. S. H. Istepanian, and Y. H. Song, "Microarray image enhancement by denoising using stationary wavelet transform," *IEEE Trans. Nanobioscience*, vol. 2, no. 4, pp. 184–189, 2003, doi: 10.1109/TNB.2003.816225.

[3] D. A. Adjeroh, Y. Zhang, and R. Parthe, "On denoising and compression of DNA microarray images," *Pattern Recognit.*, vol. 39, no. 12, pp. 2478–2493, 2006, doi: 10.1016/j.patcog.2006.02.019.

[4] C. Niu, H. Zhang, and L. Li, "Microarray Fluorescence Image Processing and Analysis," in *Proc. IEEE Int. Conf. Manipulation, Manufacturing and Measurement on the Nanoscale (3M-NANO)*, 2024, pp. 51–54, doi: 10.1109/3M-NANO61605.2024.10769626.

[5] N. A. Golilarz, I. Dehzangi, and K. Rahimi, "Optimized Adaptive Based Method for MR Image Denoising," in *Proc. IEEE 16th Int. Conf. Computational Intelligence and Communication Networks (CICN)*, 2024, pp. 976–983, doi: 10.1109/CICN63059.2024.10847356.

[6] A. Petrov and S. Shams, "Microarray Image Processing and Quality Control," *J. VLSI Signal Process. Syst. Signal Image Video Technol.*, vol. 38, no. 3, pp. 211–226, 2004, doi: 10.1023/B:VLSI.0000042488.08307.ad.

[7] K. Marias *et al.*, "Microarray Image Denoising Using a Two-Stage Multiresolution Technique," in *Proc. IEEE Int. Conf. Bioinformatics and Biomedicine*, 2007, pp. 383–389, doi: 10.1109/BIBM.2007.32.

[8] P. Kaur, G. Singh, and P. Kaur, "A Review of Denoising Medical Images Using Machine Learning Approaches," *Curr. Med. Imaging Rev.*, vol. 14, no. 5, pp. 675–685, 2018, doi: 10.2174/1573405613666170428154156.

[9] R. K. Arunakumari, K. A. Mendhurwar, and K. Kakumani, "Microarray Image Denoising using Independent Component Analysis," *Int. J. Comput. Appl.*, vol. 1, no. 11, pp. 87–93, 2010, doi: 10.5120/234-388.

[10] N. Samsudin, R. Hashim, and N. E. Abdul Khalid, "Denoising and block gridding of microarray image using mathematical morphology," in *Proc. 7th Int. Conf. Computing and Convergence Technology (ICCCT)*, 2012, pp. 230–235. [Online]. Available: `https://ieeexplore.ieee.org/document/6530332`

[11] L. Srinivasan, Y. Rakvongthai, and S. Oraintara, "Microarray Image Denoising Using Complex Gaussian Scale Mixtures of Complex Wavelets," *IEEE J. Biomed. Health Inform.*, vol. 18, no. 4, pp. 1423–1430, 2014, doi: 10.1109/JBHI.2014.2318279.

[12] R. S. Thakur, S. Chatterjee, R. N. Yadav, and L. Gupta, "Image De-Noising With Machine Learning: A Review," *IEEE Access*, vol. 9, pp. 93338–93363, 2021, doi: 10.1109/ACCESS.2021.3092425.

[13] M. M. Dhas and N. S. Singh, "Breast Cancer Diagnosis Using Majority Voting Ensemble Classifier Approach," *J. Soft Comput. Data Min.*, vol. 5, no. 1, pp. 152–169, 2024, doi: 10.30880/jscdm.2024.05.01.013.

[14] A. Mastrogianni, E. Dermatas, and A. Bezerianos, "Microarray Image Denoising using Spatial Filtering and Wavelet Transformation," in *Proc. 13th Int. Conf. Biomed. Eng.*, Springer, 2009, pp. 594–597.

[15] A. S. Agnal and K. Mala, "Noise Removal From Microarray Images Using Maximum a Posteriori Based Bivariate Estimator," *Int. J. Image Graphics Signal Process.*, vol. 5, no. 1, pp. 32–39, 2013, doi: 10.5815/ijigsp.2013.01.05.

[16] M. Mastriani and A. E. Giraldez, "Microarrays denoising via smoothing of coefficients in wavelet domain," 2018. [Online]. Available: `https://arxiv.org/abs/1807.11571`

[17] G. S. C. Kumar, R. K. Kumar, G. A. Naidu, and J. Harikiran, "Noise removal in microarray images using variational mode decomposition technique," *Telkomnika*, vol. 15, no. 4, pp. 1750–1756, 2017, doi: 10.12928/TELKOMNIKA.v15i4.5375.

[18] S. Arumugam, B. Yohannis, J. Uthayakumar, and S. Sivakumar, "Restoration of Noisy Microarray Images using Filtering Techniques," *Annals of RSCB*, vol. 25, no. 4, pp. 21095–21106, 2021. [Online]. Available: annalsofrscb.ro/index.php/journal/article/view/10160

[19] C. Gopalappa, T. K. Das, S. Enkemann, and S. Eschrich, "Removal of hybridization and scanning noise from microarrays," *IEEE Trans. Nanobioscience*, vol. 8, no. 3, pp. 210–218, 2009, doi: 10.1109/TNB.2009.2029100.

[20] A. Zifan, M. H. Moradi, and S. Gharibzadeh, "Microarray image enhancement by denoising using decimated and undecimated multiwavelet transforms," *Signal Image Video Process.*, vol. 4, no. 2, pp. 177–185, 2010, doi: 10.1007/s11760-009-0109-4.

[21] R. Ren *et al.*, "Speckle Noise Removal in Image-based Detection of Refractive Index Changes in Porous Silicon Microarrays," *Sci. Rep.*, vol. 9, no. 1, p. 15001, 2019, doi: 10.1038/s41598-019-51435-y.

[22] B. S. Gowri, S. A. H. Nair, and K. P. S. Kumar, "Hybrid arithmetic optimization algorithm with deep transfer learning based microarray gene expression classification model," *Int. J. Inf. Technol.*, vol. 16, no. 6, pp. 3923–3928, 2024, doi: 10.1007/s41870-024-01901-2.

[23] S. Elavaar Kuzhali and D. S. Suresh, "Collaborative Priors with SVD for Denoising of cDNA Microarray Images," *Indian J. Sci. Technol.*, vol. 12, no. 37, pp. 1–15, 2019, doi: 10.17485/ijst/2019/v12i37/147036.

[24] P. Nandihal, V. Bhat, and J. Pujari, "Application of FFDNET for Image Denoising On Microarray Images," *Int. J. Recent Technol. Eng. (IJRTE)*, vol. 8, pp. 2691–2694, 2019, doi: 10.35940/ijrte.C4950.098319.

[25] R. Sunitha and H. B. Phani Raju, "Evolutionary Tool for Denoising DNA Microarray Images Using CNN," in *Microelectronics, Communication Systems, Machine Learning and Internet of Things*, Springer, 2023, pp. 193–201.

[26] A. Mohandas, S. M. Joseph, and P. S. Sathidevi, "An Autoencoder based Technique for DNA Microarray Image Denoising," in *Proc. Int. Conf. Communication and Signal Processing (ICCSP)*, 2020, pp. 1366–1371, doi: 10.1109/ICCSP48568.2020.9182265.

[27] J. Lehtinen *et al.*, "Noise2Noise: Learning Image Restoration without Clean Data," 2018, doi: 10.48550/arXiv.1803.04189.

[28] A. Krull, T.-O. Buchholz, and F. Jug, "Noise2Void - Learning Denoising From Single Noisy Images," in *Proc. IEEE/CVF Conf. Computer Vision and Pattern Recognition (CVPR)*, 2019, pp. 2124–2132, doi: 10.1109/CVPR.2019.00223.

[29] D. Ulyanov, A. Vedaldi, and V. Lempitsky, "Deep Image Prior," *Int. J. Comput. Vis.*, vol. 128, no. 7, pp. 1867–1888, 2020, doi: 10.1007/s11263-020-01303-4.

[30] N. V. Orlov *et al.*, "Automatic classification of lymphoma images with transform-based global features," *IEEE Trans. Inf. Technol. Biomed.*, vol. 14, no. 4, pp. 1003–1013, 2010, doi: 10.1109/TITB.2010.2050695.

[31] J. Liu *et al.*, "Speckle noise reduction for medical ultrasound images based on cycle-consistent generative adversarial network," *Biomed. Signal Process. Control*, vol. 86, p. 105150, 2023, doi: 10.1016/j.bspc.2023.105150.

[32] K. Zhang, W. Zuo, Y. Chen, D. Meng, and L. Zhang, "Beyond a Gaussian Denoiser: Residual Learning of Deep CNN for Image Denoising," *IEEE Trans. Image Process.*, vol. 26, no. 7, pp. 3142–3155, 2017, doi: 10.1109/TIP.2017.2662206.